

## Morphogenesis of growing amorphous films

Stefan J. Linz, Martin Raible, Peter Hänggi

### Angaben zur Veröffentlichung / Publication details:

Linz, Stefan J., Martin Raible, and Peter Hänggi. 2003. "Morphogenesis of growing amorphous films." In *Interface and Transport Dynamics: Computational Modelling*, edited by Heike Emmerich, Britta Nestler, and Michael Schreckenberg, 103–18. Berlin: Springer.  
[https://doi.org/10.1007/978-3-662-07969-0\\_9](https://doi.org/10.1007/978-3-662-07969-0_9).



# Morphogenesis of Growing Amorphous Films

Stefan J. Linz, Martin Raible and Peter Hänggi

Theoretische Physik I, Institut für Physik,  
Universität Augsburg, 86135 Augsburg, Germany

**Abstract.** In a first part of this paper, we survey the conceptional and methodological background of the stochastic field equations approach to model surface growth processes. In the second part, we focus on recent progress in the modeling of such equations for the specific case of vapor deposited amorphous thin films that allow for a quantitative validation with experimental data.

## 1 Introduction

The fundamental physical laws governing the macroscopic and the microscopic world are, in principle, rather simple. Nevertheless, nature is able to create a highly complicated and structured world on the basis of these laws. Unraveling the hidden rules of nature how to fabricate such complex systems, i.e. systems being built up of many interacting constituents and exhibiting a complicated overall behavior that is not at all evident from the known underlying interaction between the individual constituents, has developed into a central area of current research in physics.

The morphogenesis or structure formation of growing surfaces and interfaces due to deposition processes constitutes a specific and nonetheless paradigmatic example of such a complex system [1,2]. Focussing on atomic deposition processes, the interplay of two individual components, i.e. atoms or molecules of the typical size of  $10^{-1}\text{nm}$ , is basically determined by their electromagnetic interaction. This, however, does not give us immediate insights into the deposition processes of particles when they arrive at a surface profile of already collectively condensed particles. It is not at all obvious how to theoretically understand the plethora of different, experimentally observed surface structures that can be created by the variety of deposition methods, deposition conditions and specific type of particles. In this context, vapor deposited amorphous films exhibit the spectacular fact of building up surface patterns with some intrinsic regularity or periodicity on scales of the order of 10nm if the film thickness reaches values of several hundred nanometers [3–5].

Even if one were able to simulate the corresponding full ab-initio many-particle problem on square areas of the corresponding size and for correspondingly long deposition times, this would not directly lead to physical insights into the underlying physical phenomena happening on the mesoscale. In the last fifteen years, an alternative approach to study surface growth phenomena [1,2,6,7] basically pioneered by the seminal work of Kardar, Parisi and Zhang

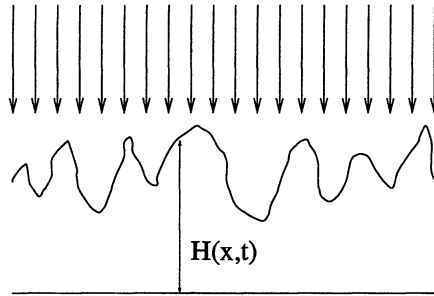


**Fig. 1.** Sketch of a representative deposition process: Particles from the incoming flux (denoted by the arrows) are deposited on the rugged surface and contribute to the spatio-temporal evolution of the surface.

[8] has attracted considerable interest and developed into a significant branch of surface physics. Here, the primary ideas are to consider the surface structure as a continuous two-dimensional manifold on a superatomic level as, for instance, represented by scanning tunneling microscopy images and then to model its spatio-temporal evolution by means of stochastic field equations (SFEs) that incorporate the relevant mesoscopic relaxation mechanisms of the deposited particles.

The focus of this work is twofold. In section 2, we critically review the basic strategies of the SFE approach for spatio-temporally evolving surface morphologies and put some emphasis on the pattern forming aspect of such equations. In section 3, we specifically apply this method to the problem of amorphous thin film growth by physical vapor deposition. We review and extend recent investigations that lead, by comparison with experimental data, to a rather complete picture of the significant relaxation phenomena and, most importantly, to an elementary description of the vapor deposition process in form of a minimal deposition equation.

## 2 Basic Concepts

**General strategy.** As starting point, we present here a synoptic account of the framework of stochastic field equations (SFEs) to model surface morphologies (for a thorough overview see Refs. [2,7]) including the clarification of some misconceptions in the literature. The general idea of the SFE approach is comparatively straightforward: A generally spatio-temporally varying flux of particles given by  $I(\mathbf{x}, t)$  reaches the surface (cf. also Fig. 1), the particles from the beam are deposited at the surface and then undergo various surface diffusion processes until they arrive at their final position. The growing layer built up by the deposited particles forms a spatio-temporally evolving free surface that is characterized by its *height* or *morphology*  $H(\mathbf{x}, t)$  at time  $t$  and the location  $\mathbf{x} = (x, y)$  measured with respect to coordinates of the initially

flat surface  $H(\mathbf{x}, 0) = 0$ . The SFE approach disregards the microscopic details of the particle arrangement and interaction at the surface and considers the growth process on a slightly larger length scale, the meso- or nanoscale, where the (coarse-grained) surface morphology  $H(\mathbf{x}, t)$  can be regarded as a field variable evolving continuously in space and time. Then, the rate of change of the surface height  $H(\mathbf{x}, t)$  can be expressed in form a partial differential equation

$$\partial_t H(\mathbf{x}, t) = G[\nabla H, \dots] + I(\mathbf{x}, t) \quad (1)$$

where the functional  $G[\nabla H, \dots]$  depends only on spatial derivatives of  $H$  and their nonlinear combinations and comprises all physical mechanisms leading to growth and relaxational processes at the surface. Writing down (1), three fundamental symmetry requirements [2] for surface growth processes have been already incorporated: (i) no dependence of (1) on the specific choice of the origin of time implying *invariance under translation in time*, (ii) no dependence of (1) on the specific choice of the origin of the coordinate system implying *invariance under translation in the direction perpendicular to the growth direction*, and (iii) no dependence of (1) on the specific choice of the origin of the  $H$ -axis implying *invariance under translation in growth direction*. These symmetry requirements on the evolution equation (1) exclude any explicit dependence of the functional  $G[\dots]$  on the time  $t$ , the spatial position  $\mathbf{x}$ , and the height  $H$ , respectively. Note, however, that these symmetry requirements do not necessarily apply to the solutions  $H(\mathbf{x}, t)$  of (1), too.

It is worthwhile noting that (1) contains several implicit assumptions: (i) the relaxation processes are local in space, (ii) no, in principle possible changes in bulk of the already built-up layer are taken into account, (iii) in order to guarantee single-valuedness of  $H(\mathbf{x}, t)$ , no overhangs in the evolving surface structure are allowed, and (iv) to fulfill moderate existence and uniqueness requirements for  $H(\mathbf{x}, t)$ , the (coarse-grained) surface profile can have at most some cusps with a *non-zero* opening angle.

**How does stochasticity enter into (1)?** In many physical applications such as vapor deposition experiments [3–5], the deposition flux is basically constant with some small superimposed spatio-temporal variations resulting from the particle source. As a consequence, the deposition flux can be split into a spatio-temporally constant mean deposition flux  $F$  and a fluctuating part  $I(\mathbf{x}, t) = F + \eta(\mathbf{x}, t)$ . As a simplest model for the generally not well-known fluctuations  $\eta(\mathbf{x}, t)$  one usually uses spatio-temporal Gaussian white noise determined by  $\langle \eta(\mathbf{x}, t) \rangle_\eta = 0$  and  $\langle \eta(\mathbf{x}, t) \eta(\mathbf{x}', t') \rangle_\eta = 2D \delta(\mathbf{x} - \mathbf{x}') \delta(t - t')$ . Here,  $\langle \dots \rangle_\eta$  denotes the ensemble average, and  $D$  the fluctuation strength. Since the mean deposition flux  $F$  is constant it also proves useful to introduce the height profile  $h(\mathbf{x}, t) = H(\mathbf{x}, t) - Ft$  in the frame comoving with the velocity  $F$ . Then, (1) simplifies to

$$\partial_t h = G[\nabla h] + \eta(\mathbf{x}, t). \quad (2)$$

As an aside, we note that the method leading to (2) also works if the mean deposition flux  $F(t)$  contains an experimentally predetermined dependence on time  $t$ . Then one straightforwardly arrives at (2) if the definition  $h(\mathbf{x}, t) = H(\mathbf{x}, t) - \int_0^t F(t') dt'$  is used.

**How to specify the functional  $G[.]$ ?** As explained before, all physics of the growth process is hidden in the functional  $G[.]$ . So, the variety of different experimentally observable surface structures must be directly related to the specific functional form of  $G[.]$ . Basically two approaches are used in the literature. One way is to select known physical relaxation mechanisms (for collection of such mechanisms see e.g.[2]) that are considered to be relevant for the specific system, combines them and tries to compare the outcome with experimental data. This method has the drawback of being non-systematic. Another way is to start from the guiding principle of simplicity of the functional form of  $G[.]$  combined with further symmetry requirements for the specifically considered system and a series expansion of  $G[.]$  in small gradients of  $h$  up to some given order. In this case, one obtains a systematic skeleton of the functional form of the SFE; it is, however, not directly evident how to relate all the terms to underlying growth and relaxation processes.

In the remainder of this section, we focus on deposition processes that also possess *invariance under rotation and reflection* in the plane perpendicular to the growth direction. An example for such processes is amorphous growth where the isotropy of the amorphous phase implies such an invariance. This symmetry immediately excludes any odd derivatives of  $h$  in  $G$  and implies that  $\nabla$ -operators entering the various contributions in  $G$  must be multiplied in couples by scalar multiplication. Assuming that all surface relaxation processes are local, we finally expand the functional  $G$  in a power series in all possible spatial derivatives of  $h$  and keep only the terms that are linear or quadratic in  $h$  and only possess a maximum of four  $\nabla$ -operators. As a result of the afore-mentioned symmetries, the deterministic part of (2) can only consist of the terms  $\nabla^2 h$ ,  $(\nabla h)^2$ ,  $\nabla^4 h$ ,  $\nabla^2(\nabla h)^2$ ,  $(\nabla^2 h)^2$ , and  $\nabla \cdot [(\nabla h)(\nabla^2 h)]$ . The last term can be slightly rearranged in the form

$$\nabla \cdot [(\nabla h)(\nabla^2 h)] = \frac{1}{2} \nabla^2 (\nabla h)^2 + 2M \quad (3)$$

with

$$M = \det \begin{pmatrix} \partial_x^2 h & \partial_y \partial_x h \\ \partial_x \partial_y h & \partial_y^2 h \end{pmatrix}. \quad (4)$$

Consequently, a *systematic* expansion of the functional form of the growth equation (1) that takes into account (i) all afore-mentioned symmetries and (ii) all admissible combinations of terms being linear or quadratic in  $h(\mathbf{x}, t)$  and containing up to a maximum of four  $\nabla$ -operators is given explicitly by

[9]

$$\begin{aligned} \partial_t h = & a_1 \nabla^2 h + a_2 \nabla^4 h + a_3 \nabla^2 (\nabla h)^2 \\ & + a_4 (\nabla h)^2 + a_5 (\nabla^2 h)^2 + a_6 M + \eta. \end{aligned} \quad (5)$$

Eq.(5) constitutes the main result of this section.

**Some general remarks.** Equation (5) consists of two linear terms and four nonlinear terms in  $h$ . The term being proportional to  $a_6$  becomes zero in the one-dimensional limit. This shows the principal problem that one-dimensionally motivated surface growth equations cannot be carried over to the two-dimensional case by simply replacing  $\partial_x \rightarrow \nabla$ . Moreover, it is interesting to note that Lai and Das Sarma [10] have also attempted to derive the leading order functional form of a growth equation using isotropy and the fact that the functional  $G$  in (2) is a scalar. Their result, however, significantly differs from (5) since the terms  $a_5 (\nabla^2 h)^2$  and  $a_6 M$  are missing. Therefore, we conclude that Lai and Das Sarma's growth equation [10] represents an inconsistent systematic expansion since the terms  $(\partial_x^2 h)(\partial_y^2 h) - (\partial_x \partial_y h)^2$  and  $(\partial_x^2 h)^2 + (\partial_y^2 h)^2 + 2(\partial_x^2 h)(\partial_y^2 h)$  are not properly taken into account.

The growth equation (5) contains several known limiting cases. The limit  $a_i = 0$  for  $i = 1, \dots, 6$ ,  $\partial_t h = \eta$ , is considered as an appropriate model for random deposition [2]. Setting  $a_i = 0$  for  $i = 2, \dots, 6$ ,  $\partial_t h = a_1 \nabla^2 h + \eta$ , yields the Edwards-Wilkinson (EW) equation originally motivated in the context of granular systems [11]. The limit  $a_i = 0$  for  $i = 2, 3, 5, 6$ , determines the Kardar-Parisi-Zhang (KPZ) equation,  $\partial_t h = a_1 \nabla^2 h + a_4 (\nabla h)^2 + \eta$ , being the paradigm for a stochastic roughening process [8]. Finally, the limit  $a_i = 0$  for  $i = 3, 5, 6$ ,  $\partial_t h = a_1 \nabla^2 h + a_2 \nabla^4 h + a_4 (\nabla h)^2 + \eta$ , leads to the stochastic version of the Kuramoto-Sivashinsky (KS) equation [12].

**Pattern forming aspects.** From the viewpoint of nonlinear dynamics, the KPZ equation and the KS equation can be considered as antipodal paradigms although they only differ by the term  $\nabla^4 h$ . This can be seen from the linearized version of (5) that dominates the initial stages of the growth process. Neglecting any stochasticity for the moment, inserting a solution or mode ansatz  $h(\mathbf{x}, t) = h_0 \exp(i\mathbf{k} \cdot \mathbf{x}) \exp(\sigma t)$  into  $\partial_t h = a_1 \nabla^2 h + a_2 \nabla^4 h$  directly leads to the dispersion relation for the growth rate,  $\sigma(k) = -a_1 k^2 + a_2 k^4$ , with  $k = |\mathbf{k}|$  being the modulus of the wave vector  $\mathbf{k}$ . Depending on the sign of the coefficients  $a_1$  and  $a_2$ , four main types of behavior can be distinguished. For  $a_1 > 0$  and  $a_2 \leq 0$ , all modes are damped with time, whereas for  $a_1 < 0$  and  $a_2 \geq 0$  all modes grow with time and they grow the faster, the larger the wave number is. If  $a_1 > 0$  and  $a_2 > 0$ , then all modes beyond the threshold  $k_T = \sqrt{a_1/a_2}$  grow. The most important case, however, occurs if  $a_1 < 0$  and  $a_2 < 0$ . Then, only wave numbers  $k$  in the range  $0 \leq k \leq \sqrt{a_1/a_2}$  can grow with time and, moreover, there is a fastest growing mode  $k_m = \sqrt{a_1/2a_2}$  that dominates the evolution of  $h$ . The latter result tells us that, at least for stages where the linearized version of the KS

equation is sufficient, a pattern with an underlying periodicity dominated by  $k_m$  develops. This growth mechanism disappears in the KPZ-type limit when  $a_2$  is set to zero. Physically interesting behavior of the KPZ equation appears when  $a_1 > 0$ . Then, the collaborate effect of the noise and the nonlinearity leads to a stochastic roughening of the surface with self-affine character [2]. The noisy KS equation for  $a_1 > 0$  and  $a_2 < 0$  leads to a similar behavior. If, however,  $a_1 < 0$  and  $a_2 < 0$ , the pattern forming mechanism dominates (for small enough noise amplitudes) the early stages of the growth process. The role of the entering nonlinearity is to modify the pattern at later stages of the growth process.

Besides the invariances already invoked for its derivation, the growth equation (5) possesses an interesting additional symmetry: It remains invariant under the combined transformation

$$\{h, a_3, a_4, a_5, a_6\} \rightarrow \{-h, -a_3, -a_4, -a_5, -a_6\}. \quad (6)$$

As a consequence, one has to expect that a simultaneous change of the sign of the coefficients  $a_3, a_4, a_5, a_6$  belonging to the nonlinear terms in (5) only leads to an inversion of the surface profile  $h(\mathbf{x}, t)$  about  $h = 0$ . Note, however, that (5) does *not* possess mirror symmetry about  $h = 0$ , i.e. it does not fulfill the up/down invariance  $h \rightarrow -h$  (without inversion of the signs of the nonlinear coefficients). This already implies some degree of asymmetry of the resulting surface profile  $h(\mathbf{x}, t)$ .

**Conservative growth processes.** A frequently invoked further requirement on surface growth equations [2,7] is that the functional  $G$  should be represented by the divergence of a surface current,  $G = -\nabla \cdot \mathbf{j}_G(\nabla h)$  if no desorption of particles can occur. Such an assumption directly rules out the appearance of a KPZ term  $(\nabla h)^2$  and the term  $(\nabla^2 h)^2$  in  $G$ . It also implies that the spatial and ensemble averaged height is related to the deposition flux by  $\langle\langle H(\mathbf{x}, t) \rangle\rangle_{\mathbf{x}} = Ft$  or, equivalently, that  $\langle\langle h(\mathbf{x}, t) \rangle\rangle_{\mathbf{x}} = 0$  holds. The afore-mentioned assumption, however, also implicitly implies that no coarse-grained *density* variations can occur. In the presence of local density variations, a discussion starting from the condition that no incoming particles are lost (cf. the following section) can lead to a KPZ term  $(\nabla h)^2$  and a term  $(\nabla^2 h)^2$  and, therefore, also to a nonzero *excess velocity*  $v = \langle\langle \partial_t h \rangle\rangle_{\mathbf{x}} = \langle\langle a_4(\nabla h)^2 + a_5(\nabla^2 h)^2 \rangle\rangle_{\mathbf{x}}$  of the surface profile  $h(\mathbf{x}, t)$ .

**How to make contact with experimental results?** Modern experimental investigation tools such as scanning tunneling microscopy combined with image processing allow for a detailed resolution of the surface morphology and its spatio-temporal evolution [3–5]. Since the obtained data set is too immense and the data also contain some degree of stochasticity due to the small deposition noise resulting from the particle source, the *height-height-correlation function*

$$C(r, t) = \langle\langle [H(\mathbf{x} + \mathbf{r}, t) - \langle H \rangle_{\mathbf{x}}][H(\mathbf{x}, t) - \langle H \rangle_{\mathbf{x}}] \rangle\rangle_{\mathbf{x}, |\mathbf{r}|=r} \quad (7)$$

determines an appropriate quantitative statistical measure for the information on height variations and lateral correlations. In (7),  $\langle \dots \rangle_\eta$  represents an average over different samples (ensemble average),  $\langle \dots \rangle_{\mathbf{x}} = L^{-2} \int_0^L d^2x \dots$  the spatial average over a sample area of size  $L^2$ , and  $\langle H \rangle_{\mathbf{x}} = \langle H \rangle_{\mathbf{x}}(t) = \langle H(\mathbf{x}, t) \rangle_{\mathbf{x}}$  the spatially averaged surface profile at time  $t$ . The height-height-correlation function  $C(r, t)$  contains the two most important global quantities that characterize the surface morphology: (i) The *correlation length*  $R_c(t)$  that is given by the first maximum of  $C(r, t)$  for non-zero  $r$ , i.e. by  $R_c(t) = \min\{r > 0 | \partial_r C(r, t) = 0, \partial_r^2 C(r, t) < 0\}$ , and, therefore, determines the typical length scale over which height fluctuations are correlated, and (ii) the *surface roughness*  $w(t)$  or root mean square deviation of the relative height fluctuations that is determined by the  $r = 0$ -limit of  $C(r, t)$ ,  $w^2(t) = C(0, t)$ . Another often used statistical measure of the surface morphology is the *spectral power density* that is determined by

$$C(\mathbf{k}, t) = C(|\mathbf{k}|, t) = \mathcal{F}[C(r, t)] = \mathcal{F}[C(|\mathbf{r}|, t)] \quad (8)$$

where  $\mathcal{F}[\dots]$  represents the two-dimensional Fourier transform with respect to the wave vector  $\mathbf{k}$ . As a minimum requirement for a successful modeling attempt of the spatio-temporal evolution of  $H(\mathbf{x}, t)$ , the validation of the temporal evolution of  $R_c(t)$  and  $w(t)$  in comparison with the available experimental data needs to be achieved.

### 3 Deposition Equation for Thin Film Growth

In this section, we specifically focus on the growth of solid amorphous films generated by physical vapor deposition under normal incidence of the particle flux that is important e.g. in the context of coating and the manufacturing of thin glassy ZrAlCu films and has recently attracted interest [3–5,13] in materials science. We review and partly extend some major results obtained in recent works [13–16] on the development and detailed analysis of a minimal model in form of a SFE that (i) appropriately describes the spatio-temporal evolution of such amorphous surface growth processes and (ii) stands the test of a quantitative comparison with available experimental data [3–5,13]. From the theoretical point of view, amorphous film growth constitutes a particularly attractive testing ground for a *quantitative* comparison of experimental data and theoretical approaches since (i) there are not any long range ordering phenomena (as in epitaxial growth processes) to be expected, (ii) the effect of terrace formation and, therefore, the Ehrlich-Schwoebel effect being significant for epitaxial growth processes are absent, and (iii) the growing film should be spatially isotropic. As an appropriate starting point, we can directly use the general form (5) that contains all basic symmetries relevant for the vapor deposition process.

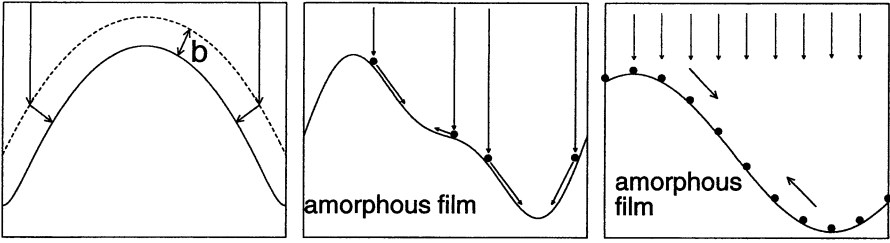


**Fig. 2.** Microscopic effects of amorphous surface growth. Left part: Inflection of particles due to interatomic interaction. Middle part: Surface diffusion of deposited particles due to surface relaxation. Right part: Equilibration of the inhomogeneous particle concentration due to the geometry of the surface.

**Physics behind the growth equation.** Guided by the principle that any mathematically admissible term might have some physical significance, we next relate all terms appearing in the growth equation (5) to the four competing microscopic mechanisms

- surface tension [18]
- concentration equilibration of deposited particles [19,20]
- steering of arriving particles [14]
- inhomogeneous density distribution [14,15]

that, as we shall see in the next section, seem to dominate physical vapor deposition and are all, at least at some stages of the growth process, important. Also the signs and the order of magnitude estimates of some coefficients in (5), as well as a physically motivated simplification of (5) are obtained.

The linear term proportional to  $a_2$  in (5) can be interpreted as the result of a type of a microscopic surface tension effect as originally suggested by Mullins [18]. The basic idea behind this effect (cf. also the middle part of Fig. 2) is that the just deposited particles favorably move to positions at the surface that have positive curvature  $\nabla^2 h > 0$  since there, the already condensed surface particles form a local vicinity with higher binding energy. This gives rise to a diffusion current  $\mathbf{j}_m \propto \nabla(\nabla^2 h)$  that, depending on the local curvature, can be uphill or downhill. The divergence of this current,  $-\nabla \cdot \mathbf{j}_m = a_2 \nabla^4 h$ , contributes to the surface evolution in (5) with  $a_2$  being necessarily negative. This term basically tries to minimize the area of the surface and, as a consequence, to smooth the surface morphology.

The nonlinear term proportional to  $a_3$  can be related to the tendency of equilibrating the non-homogeneous concentration  $c$  of the deposited particles just after arriving at the surface. This effect has originally been suggested by Villain [19] (cf. also [20]). The underlying reason is of purely geometric nature. Although the deposition flux is basically homogeneous, more particles per surface area arrive at positions with a small or zero modulus of slope  $\nabla h$

than at positions being strongly inclined with respect to the particle beam, cf. also the right part of Fig. 2. Therefore, the local concentration of the diffusing particles right after the deposition is not constant, but is weighted by the local slope of the surface,  $c \propto 1/\sqrt{1 + (\nabla h)^2}$ , or in a small gradient expansion,  $c \propto 1 - \frac{1}{2}(\nabla h)^2$ . Then, the tendency to equilibrate the concentration is reflected by a diffusion current  $\mathbf{j}_c \propto -\nabla c \propto \nabla(\nabla h)^2$ , or, after taking the divergence, by the term  $-\nabla \cdot \mathbf{j}_c = a_3 \nabla^2(\nabla h)^2$  that contributes to the height changes in (5). Obviously, concentration equilibration requires that the coefficient  $a_3$  is negative and also tries to smooth the surface morphology. A simple dimensional argument leads to an estimate for  $a_3$ . Equation (5) implies that the coefficient  $a_3$  has the dimension of length<sup>3</sup>/time. The magnitude of  $a_3$  necessarily depends on the deposition flux  $F$  that possesses the dimension of length/time and the mean diffusion length  $l$  which is the only relevant length scale determining this process. The only combination of  $F$  and  $l$  leading to the correct dimension of  $a_3$  is  $Fl^2$ . Therefore, one expects  $a_3 \propto -Fl^2$ . A thorough discussion of the concentration equilibration [14] supports this argument and yields the explicit relation  $a_3 = -\frac{1}{8}Fl^2$ . Moreover, one expects that the typical magnitude of  $l$  is of the order of several atom diameters.

The two terms in (5) that are proportional to  $a_1$  and  $a_6$  can microscopically be related to the steering of the arriving particles. Here, the basic idea [14] is that the particles from the beam experience close to the growing surface a deflection due to the interatomic attractive interaction with the already condensed surface particles. As a consequence, the particles do not hit the surface perpendicular to the substrate orientation, but perpendicular to the surface itself. This implies that more particles arrive at positions at the surface with negative curvature,  $\nabla^2 h < 0$ , than at positions with positive curvature  $\nabla^2 h > 0$ . Effectively, this leads to a tendency to roughen the surface morphology. We refer to Ref. [21] for experimental indications of the relevance of this effect. To model this scenario in a dynamical way [14], we use the idealization that the particles undergo a change of direction only after reaching a critical distance  $b$ , the effective range of the interaction, from the surface and are then attracted such that they arrive perpendicular to the surface, cf. the left part of Fig. 2. A detailed mathematical derivation [14] using a reparametrization in the coordinates of the imaginary surface where the interaction becomes effective (cf. the dotted line in the left part of Fig. 2) and a small gradient expansion in  $h$  in fact shows that this scenario gives simultaneously rise to the two contributions  $a_1 \nabla^2 h$  and  $a_6 M$  in (5). Moreover, the coefficients  $a_1$  and  $a_6$  can be related to the mean deposition flux  $F$  and the effective range  $b$  of the interatomic interaction yielding  $a_1 = -Fb$  and  $a_6 = Fb^2$  [14]. Although  $b$  cannot be directly measured its magnitude should be typically of the order of one atomic diameter and, therefore, much smaller than the radius of the surface curvature. This implies that the term proportional to  $a_6$  is of minor relevance in comparison to the  $a_1$ -term and can be neglected. Moreover, the sign of  $a_1$  is negative.

The physical origin of the nonlinear terms proportional to  $a_4$  and  $a_5$  is determined by the potential variations of the coarse-grained density [13,14]. These terms cannot result from particle desorption since the substrate is held at room temperature and the particle energy in the vapor beam is rather low (typically of the order 0.1eV). Therefore, *all* arriving particles finally contribute to the surface growth. As a consequence, any term that cannot be recast in form of the divergence of a current in (5) arises from changes of the coarse-grained density. Assuming for the moment that the deposition noise is zero ( $\eta = 0$ ), particle conservation implies that the rate of change of the number of particles per substrate area above a given substrate location,  $C$ , is determined by a balance equation  $\partial_t C = -\nabla \cdot \mathbf{j}_C + \rho_0 F$ . Here the divergence of the current  $\mathbf{j}_C$  is given by the combination of all surface relaxation processes (cf. the afore-mentioned arguments), i.e. by  $-\nabla \cdot \mathbf{j}_C = \rho_0[a_1 \nabla^2 H + a_2 \nabla^4 H + a_3 \nabla^2 (\nabla H)^2 + a_6 M]$ , and  $\rho_0$  represents the density of the growing film in the case of a horizontal surface. Allowing for density variations at the growing surface, the rate of change of  $C$  is related to the rate of change of the height  $H$  by  $\partial_t C = \rho(\nabla H) \partial_t H$ . Here  $\rho(\nabla H)$  denotes the density at the surface. Without the incorporation of density changes ( $\rho = \rho_0 = const.$ ), there is a direct proportionality  $\partial_t C = \rho_0 \partial_t H$ . If small density variations are taken into account,  $\rho(\nabla H)$  can be expanded in the derivatives of  $H$  yielding  $\rho(\nabla H) = \rho_0[1 + q_1(\nabla H)^2 + q_2 \nabla^2 H]$  in lowest order approximation. Therefore,  $\partial_t H = \rho_0^{-1}[1 - q_1(\nabla H)^2 - q_2 \nabla^2 H] \partial_t C$  holds. Inserting this in the balance equation from above, explains the presence of the two terms  $-q_1 F(\nabla H)^2 = a_4(\nabla h)^2$  and  $-q_2 a_1(\nabla^2 H)^2 = a_5(\nabla^2 h)^2$  appearing in (5). From the physical point of view, however, density changes are primarily connected to the gradients of the surface profile reflecting the local arrangement of the particles at the surface and not so much to the surface curvature. Therefore, it is plausible to disregard the term  $a_5(\nabla^2 h)^2$  in a minimal description of the growth evolution. Since the density variations result from a widening of the mean inter-particle distances at the surface or an enlarged number of microscopic vacancies in the growing material one has to expect that they locally decrease the density implying that  $a_4 > 0$  holds.

Taking into account the afore-mentioned physical arguments, the terms  $a_5(\nabla^2 h)^2$  and  $a_6 M$  are negligible in leading order and, as a final result, we obtain the model equation for amorphous film growth [9,13–15],

$$\partial_t h = a_1 \nabla^2 h + a_2 \nabla^4 h + a_3 \nabla^2 (\nabla h)^2 + a_4 (\nabla h)^2 + \eta \quad (9)$$

with  $a_1, a_2, a_3$  being negative and  $a_4$  being positive.

Using stochastic numerical simulations of the surface growth equation (9) starting from a flat substrate (for details of the different methods see Ref. [17]), we investigate in the remainder of this contribution the evolution of the correlation length  $R_c$  and surface roughness  $w$  as a function of the experimentally measurable layer thickness  $\bar{H}$ . This quantity is determined by  $\bar{H} = \langle \langle H(\mathbf{x}, t) \rangle \rangle_{\mathbf{x}} = Ft + \langle \langle h(\mathbf{x}, t) \rangle \rangle_{\mathbf{x}}$  and is, in general, implicitly connected to the time  $t$  via the solution of (9). The latter results from the fact that

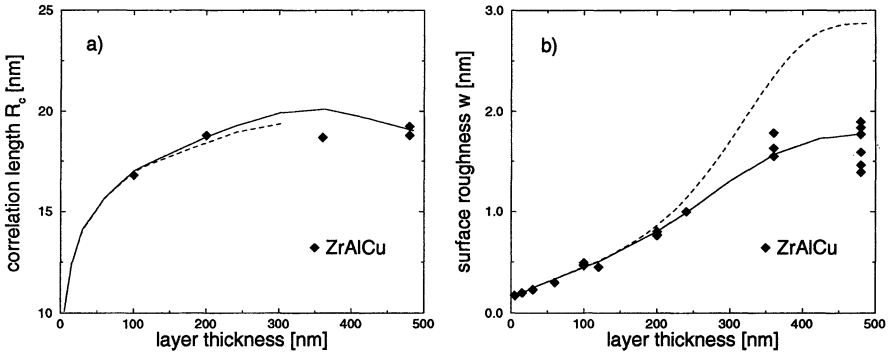


**Fig. 3.** Solid lines (dashed lines): Correlation length  $R_c$  and surface roughness  $w$  for the experimentally investigated thickness interval  $0 \leq \bar{H} \leq 480\text{nm}$  calculated from the nonlinear growth equation (9) using the parameters  $a_1 = -0.0826\text{nm}^2/\text{s}$ ,  $a_2 = -0.319\text{nm}^4/\text{s}$ ,  $a_4 = 0.055\text{nm}/\text{s}$ ,  $D = 0.0174\text{nm}^4/\text{s}$  and  $a_3 = -0.10\text{nm}^3/\text{s}$  ( $a_3 = 0\text{nm}^3/\text{s}$ ). Diamonds represent the corresponding experimental results previously published in Ref.[3,22]. This figure is taken from Ref.[13].

the surface profile generated by (9) possesses a finite excess velocity,  $v = \langle \langle \partial_t h \rangle_\eta \rangle_{\mathbf{x}} = \langle \langle a_4 (\nabla h)^2 \rangle_\eta \rangle_{\mathbf{x}}$ . Since  $a_4$  is positive the average of the surface morphology  $H(\mathbf{x}, t) = Ft + h(\mathbf{x}, t)$  grows with a faster speed than  $F$  as a result of the inhomogeneous density distribution.

**Selected results.** Here, we show that the model equation (9) is indeed able to quantitatively reproduce experimental data on the correlation length  $R_c$  and surface roughness  $w$  if the coefficients  $a_1$ ,  $a_2$ ,  $a_3$ ,  $a_4$  and  $D$  are appropriately chosen. For the specific example of the growth of  $\text{Zr}_{65}\text{Al}_{17.5}\text{Cu}_{27.5}$  films [3–5,13], a parameter estimation procedure discussed in detail in [13] yields for the coefficients in (9)  $a_1 = -0.0826\text{nm}^2/\text{s}$ ,  $a_2 = -0.319\text{nm}^4/\text{s}$ ,  $a_3 = -0.10\text{nm}^3/\text{s}$ , and  $a_4 = 0.055\text{nm}/\text{s}$  and for the strength of the deposition noise  $D = 0.0174\text{nm}^4/\text{s}$ . The experimentally determined mean deposition flux is given by  $F = 0.79\text{nm}/\text{s}$ . For this set of parameter values, we show the dependence of the correlation length  $R_c$  and surface roughness  $w$  (solid lines) on the thickness of the amorphous film in Fig. 3 and infer a very good agreement with the corresponding experimental data. For comparison, the corresponding results of the Kuramoto-Sivashinsky limit ( $a_3=0$ , dashed lines) are given. Since the correlation length ceases to exist at a film thickness of about 300nm in this limit we also conclude that both nonlinear terms proportional to  $a_3$  and  $a_4$  are necessary to reproduce the experimental data. Leaving off the term that describes the effect of density inhomogeneities,  $a_4 = 0$ , the surface roughness increases strongly with time and does not show the cross-over to a saturation at layer thicknesses of about 480nm (for more

details of this limit cf. Ref.[14,15]). Moreover, both linear terms proportional to  $a_1$  and  $a_2$  are necessary to excite the growth instability at the initial stages of the growth process [14]. Consequently, (9) must be considered as a minimal model for the growth of amorphous  $\text{Zr}_{65}\text{Al}_{7.5}\text{Cu}_{27.5}$  films.

The extrapolated parameters  $a_1$ ,  $a_2$ ,  $a_3$ ,  $a_4$ , and  $D$  also allow for microscopic estimates [13]. (i) Since  $a_1 = -Fb$ , the typical range  $b$  of the interaction between the surface atoms and the particles to be deposited is about 0.1nm, i.e. of the size of the radii (0.2nm) of the surface atoms. (ii) Since  $a_3 = -Fl^2/8$ , the diffusion length  $l$  is about 1.0nm. Consequently, the deposited particles experience a surface diffusion on a nanometer scale and do not just stick at the places where they hit the surface. (iii) If the particles arrive independently on the surface, the deposition noise is related to the particle volume  $\Omega$  and the mean deposition rate  $F$  by  $2D = F\Omega$  [14], yielding  $\Omega = 0.04nm^3$ . This is up to a factor of two the averaged particle volume of  $\text{ZrAlCu}$ . (iv) The local density of the growing film varies with the surface slope: On an inclined surface area the local density is decreased by  $\rho(\nabla h) = \rho_0/\gamma$  with  $\gamma = 1 + (a_4/F)(\nabla h)^2$  (where  $a_4/F$  is about 0.07). These finite density variations are physically compatible with the small diffusion length  $l$  of two to three atom diameters. At the layer thickness 480nm, this local density reduction  $\gamma$  (averaged over the surface) possesses a mean 1.021 and a standard deviation 0.017.

Finally, we present in Fig. 4 the dependence of the Fourier transform of the height-height correlation function,  $C(k, t)$  (see (8)), on the modulus of the wave vector for five subsequent deposition times or layer thicknesses obtained from the numerical solution of (9). Also here, our numerical simulations show a striking agreement with previously published experimental data (cf. Fig. 4 [right part] in Ref.[22] and also Fig. 3 in Ref.[23]). As in these experiments, one recovers (i) the characteristic decay proportional to  $k^{-4}$  that gives clear evidence of the importance of the Mullins term  $a_2\nabla^4 h$  in (9) and (ii) the slight buckling of  $C(k)$  for the layer thickness of 480nm and wave numbers  $k$  somewhat larger than  $10^{-1}\text{nm}^{-1}$  where in a narrow range of  $k$  a decay proportional to  $k^{-1}$  can be fitted. A detailed numerical comparison with and without the density variation term,  $a_4(\nabla h)^2$ , in (9) shows that this effect is directly related to the inclusion of density variations. Based on their experimental data (cf. Fig. 3 in Ref.[23]), Mayr and Samwer [23] have recently suggested an alternative explanation for this effect. Using the old idea tracing back to Mullins [18] that a *linear* term leading to a decay proportional to  $k^{-1}$  might be related to viscous flow in the bulk, these authors have designed a qualitative model of viscous hill coalescence to explain this feature. Since the decay of the power spectral density  $C(k, t)$  proportional to  $k^{-1}$  in a small range of  $k$  is in our analysis a direct consequence of the *nonlinear* KPZ term, it does not seem to substantiate the presence of viscous flow in the bulk. Moreover, the remark in [23] that the KPZ term,  $a_4(\nabla h)^2$ , in (9) might be interpreted as the lowest order mathematical representation of viscous hill coalescence is not convincing. If no desorption takes place and a KPZ term,

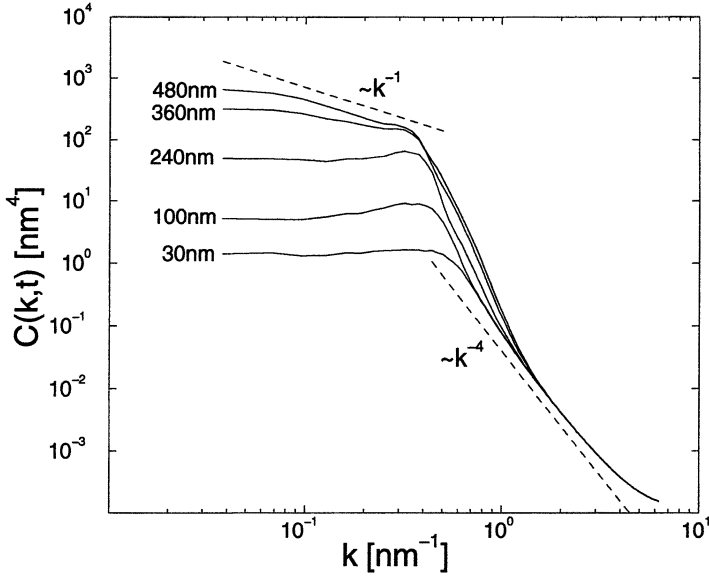


**Fig. 4.** Dependence of the Fourier transform of the height-height correlation function or power spectral density,  $C(k, t)$ , on the modulus of the wave vector for five subsequent deposition times or layer thicknesses calculated from the nonlinear growth equation (9) using the parameters  $a_1 = -0.0826\text{nm}^2/\text{s}$ ,  $a_2 = -0.319\text{nm}^4/\text{s}$ ,  $a_3 = -0.10\text{nm}^3/\text{s}$ ,  $a_4 = 0.055\text{nm}/\text{s}$  and  $D = 0.0174\text{nm}^4/\text{s}$ .

$a_4(\nabla h)^2$ , is invoked to explain experimental data, then it must be related to density variations. All other effects that are based on transport mechanisms should be expressible in terms of divergences of currents.

Next, we explore some properties of the growth process in a layer thickness range up to 2000nm that has so far not yet experimentally investigated. The results in Fig. 3 up to a layer thickness of 480nm suggest that the growth process has not yet reached a final, not necessarily stationary state. Using again the afore-mentioned parameter values, the dependence of the correlation length  $R_c$  and surface roughness  $w$  (solid lines) on the thickness of the amorphous film is shown in Fig. 5 (the dashed lines refer to the special case  $a_3=0$ ). Obviously, the surface roughness has reached an almost constant value for a layer thickness larger than 600nm that increases only very weakly as the growth process proceeds. In contrast to that, the correlation length steeply decays after reaching a maximum and then saturates in an almost constant value for a layer thickness larger than 600nm as the growth process proceeds. For further results, in particular the properties of the correlation function and the related height difference correlation function as well as visualizations of the surface morphology and a theoretical interpretation of the various stages of the growth process, we refer to Ref.[15].

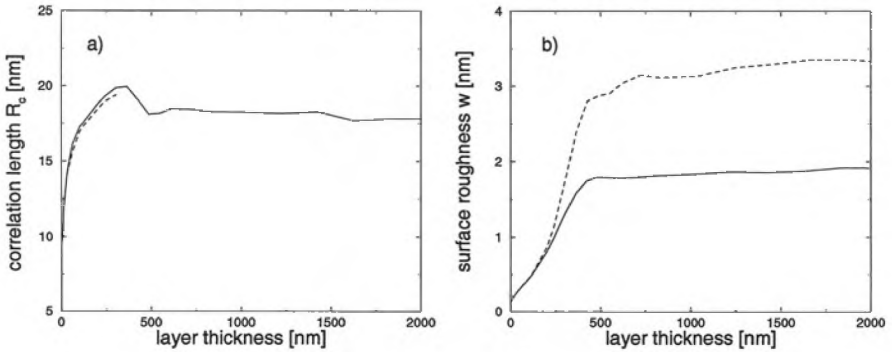


**Fig. 5.** Solid lines (dashed lines): Correlation length  $R_c$  and surface roughness  $w$  for the thickness interval  $0 \leq \bar{H} \leq 2000\text{nm}$  calculated from the nonlinear growth equation (9) using the parameters  $a_1 = -0.0826\text{nm}^2/\text{s}$ ,  $a_2 = -0.319\text{nm}^4/\text{s}$ ,  $a_3 = -0.10\text{nm}^3/\text{s}$  ( $a_3 = 0\text{nm}^3/\text{s}$ ),  $a_4 = 0.055\text{nm}/\text{s}$ , and  $D = 0.0174\text{nm}^4/\text{s}$ .

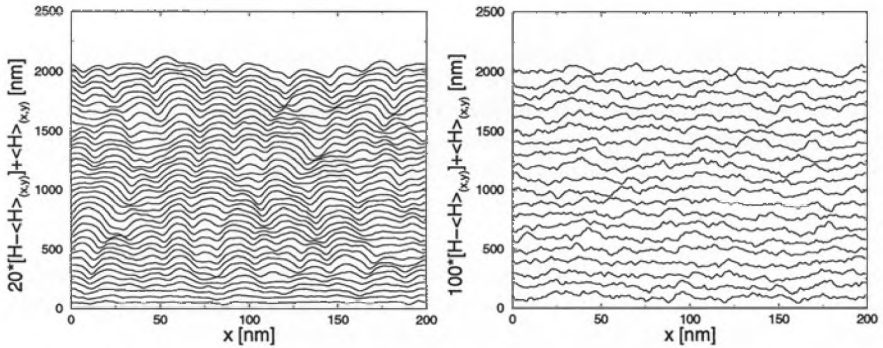


**Fig. 6.** Visualization of the cross-section of the spatio-temporal evolution of the growing surface of the film calculated from the nonlinear growth equation (9). Left part: realistic parameters for ZrAlCu  $a_1 = -0.0826\text{nm}^2/\text{s}$ ,  $a_2 = -0.319\text{nm}^4/\text{s}$ ,  $a_3 = -0.10\text{nm}^3/\text{s}$ ,  $a_4 = 0.055\text{nm}/\text{s}$ , and  $D = 0.0174\text{nm}^4/\text{s}$ ; right part: same parameters except of a sign change of  $a_1$ , i.e.  $a_1 = 0.0826\text{nm}^2/\text{s}$ .

To obtain further insight into the spatio-temporal evolution of the surface morphology, we present in the left part of Fig. 6 a representative one-dimensional cross-section of the growth of the surface profile (for  $y = 0$ ) with increasing time or layer thickness. For demonstration purposes, the relative height fluctuations have been weighted by a factor of 20 relative to the mean thickness  $\langle H \rangle_x = \langle H \rangle_{(x,y)}$ . From the left part of Fig. 6, three remarkable features can be read off. First, as the time proceeds and the layer builds up, the surface morphology develops into a predominantly almost periodic structure

with an averaged periodicity length given by the correlation length  $R_c$  and some superimposed stochastic variations. Second, the evolving mound and dip structure is asymmetric in the sense that the dips are comparatively narrow in contrast to the wide mounds. Third and most remarkably, the surface morphology does not approach a stationary profile in the thickness range  $1000\text{nm} \leq \langle H \rangle_{(x,y)} \leq 2000\text{nm}$ . Despite the fact that statistical quantities such as the correlation length and the surface roughness are almost constant in this thickness interval, the surface profile still varies significantly with time. The right part of Fig. 6 depicts (up to some scaling of the amplitudes) the evolution of the surface morphology for the same parameters *except* that the sign of the coefficient  $a_1$  has been inverted. Although this parameter set is not really physical, it shows the remarkable fact that, as a consequence of the inversion of the sign of  $a_1$ , the surface structure changes from a pattern with intrinsic regularity (depicted on the left panel of Fig. 6 with negative  $a_1$ ) to a stochastically varying profile without any regularity when  $a_1$  changes its sign (see right panel of Fig. 6). Beyond that, the roughness of the surface itself is largely reduced in comparison to the case  $a_1 < 0$ . The distinct surface evolution for positive and negative values of  $a_1$  supports our previous statements about pattern forming aspects in section 2.

## 4 Conclusions and Perspectives

Based on (i) a systematically derived minimal functional form of a growth equation being appropriate for the understanding of amorphous thin film growth, cf. equation (5), and (ii) relations of the terms occurring in the functional form (5) to underlying microscopic surface relaxation mechanisms, a quantitative agreement of the temporal evolution of the correlation length and the surface roughness of the surface morphology with experimental data can be achieved. We expect that similar quantitative agreement of experimental data and appropriately modeled SFEs for the spatio-temporal evolution of surface morphologies can also be obtained for different systems such as for crystalline growth processes or sputter deposition.

*Acknowledgement:* This work has been supported by Sonderforschungsbereich 438 (TU München/Univ. Augsburg), Project A1.

## References

1. Tong, W. M., Williams, R. S.: Kinetics of surface growth. *Annu. Rev. Phys. Chem.* **45** (1994) 401-438
2. Barabasi A.-L., Stanley, H. E. : *Fractal concepts in surface growth* (Cambridge University Press, Cambridge, 1995)
3. Reinker, B., Moske, M., Samwer, K.: Kinetic roughening of amorphous ZrAlCu films investigated in situ with scanning tunneling microscopy. *Phys. Rev. B* **56** (1997) 9887-9893

4. Mayr, S. G., Moske, M., Samwer, K.: Early stages in amorphous  $Zr_{65}Al_{7.5}Cu_{27.5}$  film growth on HOPG. *Europhys. Lett.* **44** (1998) 465-470
5. Mayr, S. G., Moske, M., Samwer, K.: Identification of key parameters by comparing experimental and simulated growth of vapor deposited amorphous  $Zr_{65}Al_{7.5}Cu_{27.5}$  films. *Phys. Rev. B* **60** (1999) 16950-16955
6. Krug, J.: Origins of scale invariances in growth processes. *Adv. Phys.* **46** (1997) 139-282
7. Marsili, M., Maritan, A., Toigo, F., Banavar, J. R.: Stochastic growth equations and reparametrization invariance. *Rev. Mod. Phys.* **68** (1996) 963-983
8. Kardar, M., Parisi, G., Zhang, Y. C.: Dynamic scaling of growing interfaces. *Phys. Rev. Lett.* **56** (1986) 889-892
9. Linz, S. J., Raible, M., Hänggi, P.: Stochastic field equation for amorphous surface growth. *Lecture Notes in Physics* **557** (2000) 473-483
10. Lai Z.-W., Das Sarma S.: Kinetic growth with surface relaxation: continuum versus atomistic models. *Phys. Rev. Lett.* **66** (1991) 2348-2351
11. Edwards S., Wilkinson D.R.: The surface statistics of a granular aggregate. *Proc. Roy. Soc. London A* **381** (1982) 17-31
12. Drotar, J. T., Zhao, Y.-P., Lu, T.-M., Wang, G.-C.: Numerical analysis of the noisy Kuramoto-Sivashinsky equation in 2 + 1 dimensions. *Phys. Rev. E* **59** (1999) 177-185
13. Raible, M., Mayr, S. G., Linz, S. J., Moske, M., Hänggi, P., Samwer, K.: Amorphous thin film growth: theory compared with experiment. *Europhys. Lett.* **50** (2000) 61-67
14. Raible, M., Linz, S. J., Hänggi, P.: Amorphous thin film growth: minimal deposition equation. *Phys. Rev. E* **62** (2000) 1691-1705
15. Raible, M., Linz, S. J., Hänggi, P.: Amorphous thin film growth: effects of density inhomogeneities. *Phys. Rev. E* **64** (2001) 031506 1-11
16. Linz, S. J., Raible, M., Hänggi, P.: Amorphous thin film growth: modeling and pattern formation. *Adv. Solid State Phys.* **41** (2001) 391-403
17. Raible, M., Linz, S. J., Hänggi, P.: Amorphous thin film growth: simulation methods for stochastic deposition equations. *Acta Phys. Pol. B* **33** (2002) 1049-1061
18. Mullins, W. W.: Theory of thermal grooving. *J. Appl. Phys.* **28** (1957) 333-339; Flattening of a nearly planar solid surface due to capillarity. *J. Appl. Phys.* **30** (1959) 77-83
19. Villain, J.: Continuum models of crystal growth from atomic beams with and without desorption. *J. Physique I* **1** (1991) 19-42
20. Moske, M.: *Mechanische Spannungen als Sonde für Schichtwachstum und Schichtreaktionen* (Habilitation thesis, Universität Augsburg, 1997)
21. van Dijken, S., Jorritsma, L. C., Poelsema, B.: Steering-enhanced roughening during metal deposition at grazing incidence. *Phys. Rev. Lett.* **82** (1999) 4038-4041
22. Mayr, S. G., Moske, M., Samwer, K.: Identification of key surface processes for vapor deposited amorphous metallic film growth. *Mater. Sci. Forum* **343-346** (2000) 221-230
23. Mayr, S. G., Samwer, K.: Model for intrinsic stress formation in amorphous thin films. *Phys. Rev. Lett.* **87** (2001) 036105 1-4